US regional tornado outbreaks and their links to spring ENSO phases and North Atlantic SST variability

Environmental Research Letters

US regional tornado outbreaks and their links to spring ENSO phases and North Atlantic SST variability

Sang-Ki Lee[1,2], **Andrew T Wittenberg**[3], **David B Enfield**[1], **Scott J Weaver**[4], **Chunzai Wang**[2] and **Robert Atlas**[2]

1 Cooperative Institute for Marine and Atmospheric Studies, University of Miami, Miami, FL, USA
2 Atlantic Oceanographic and Meteorological Laboratory, NOAA, Miami, FL, USA
3 NOAA Geophysical Fluid Dynamics Laboratory, Princeton, NJ, USA
4 Climate Prediction Center, NOAA, College Park, MD, USA

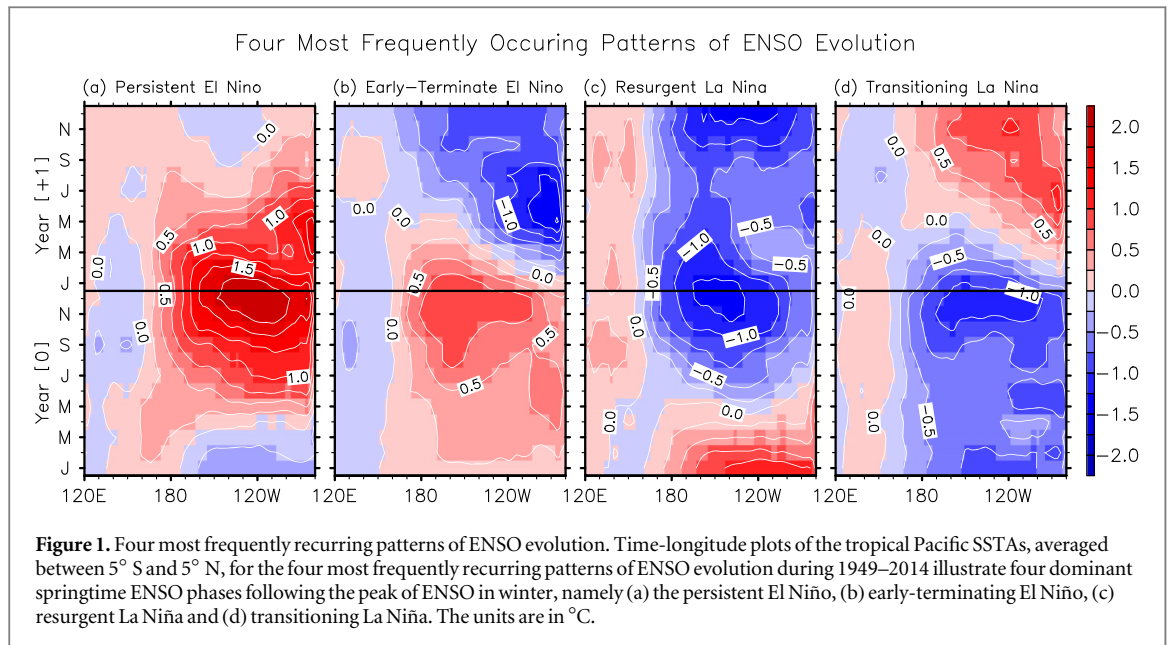E-mail: Sang-Ki.Lee@noaa.gov

Abstract

Recent violent and widespread tornado outbreaks in the US, such as occurred in the spring of 2011, have caused devastating societal impact with significant loss of life and property. At present, our capacity to predict US tornado and other severe weather risk does not extend beyond seven days. In an effort to advance our capability for developing a skillful long-range outlook for US tornado outbreaks, here we investigate the spring probability patterns of US regional tornado outbreaks during 1950–2014. We show that the four dominant springtime El Niño-Southern Oscillation (ENSO) phases (persistent versus early-terminating El Niño and resurgent versus transitioning La Niña) and the North Atlantic sea surface temperature tripole variability are linked to distinct and significant US regional patterns of outbreak probability. These changes in the probability of outbreaks are shown to be largely consistent with remotely forced regional changes in the large-scale atmospheric processes conducive to tornado outbreaks. An implication of these findings is that the springtime ENSO phases and the North Atlantic SST tripole variability may provide seasonal predictability of US regional tornado outbreaks.

1. Introduction

The latest US Natural Hazard Statistics reported that during 2005–2014 tornadoes claimed 1100 lives in the US, and caused $21.7 billion in property and crop damages (supplementary table 1). To help emergency managers, government officials, businesses and the public better prepare the resources needed to save lives and protect critical infrastructure, there is an urgent need for earlier prognosis of tornadogenesis, more effective warning systems, and an expansion of the current severe weather outlooks beyond seven days.

As summarized in a recent review [1], notable advances have been made since 2011, a year of record-breaking spring tornado outbreaks in the US, toward expanding the severe weather outlook at the National Oceanic and Atmospheric Administration beyond weather time scales [2–8]. In particular, one study [5]

showed that the majority of the extreme US tornado outbreaks in April and May during 1950–2010 were linked to a positive Trans-Niño, which typically occurs during spring following the peak of La Niña and indicates a positive zonal gradient of sea surface temperature anomalies (SSTAs) from the central tropical Pacific to the eastern tropical Pacific [9, 10]. A further analysis using an atmospheric reanalysis and modeling experiments showed that a positive Trans-Niño could enhance large-scale atmosphere conditions conducive to intense tornado outbreaks over the US via extratropical teleconnections [5]. Another study [8] showed that La Niña events persisting into spring (with March–May SSTAs in the Niño3.4 region (120°–180° W and 5° S-5° N) below −0.5 °C) could increase US tornado activity, especially over Oklahoma, Arkansas and northern Texas, and vice versa for El Niño events persisting into spring (with March–May SSTAs

Figure 1. Four most frequently recurring patterns of ENSO evolution. Time-longitude plots of the tropical Pacific SSTAs, averaged between 5° S and 5° N, for the four most frequently recurring patterns of ENSO evolution during 1949–2014 illustrate four dominant springtime ENSO phases following the peak of ENSO in winter, namely (a) the persistent El Niño, (b) early-terminating El Niño, (c) resurgent La Niña and (d) transitioning La Niña. The units are in °C.

in the Niño3.4 region above 0.5 °C). In line with these studies, a recent study [11] emphasized that the seasonal phasing of El Niño-Southern Oscillation (ENSO) is critical to its impacts on the North American low-level jets, which influence US tornado activity by controlling low-level vertical wind shear and moisture availability [3, 12].

These recent findings have identified ENSO as a potential source of seasonal predictability for US tornado activity. However, it should be noted that shortly after its peak in winter, ENSO typically decays in spring (the most active tornado season) with highly variable amplitude and spatiotemporal structure. Thus, the ENSO-related tropical Pacific SSTAs are much weaker and less coherent in spring than in winter [10]. Additionally, every ENSO event is unique in terms of its amplitude and spatial structure, particularly in spring [9, 10, 13–16]. For example, an ENSO event, while weakening during or after spring, may subsequently evolve into the onset of another ENSO event with either the same or opposite sign in the subsequent months (e.g., 1986–1987 El Niño, 1987–1988 El Niño and 1988–1989 La Niña). Hence, it is unlikely that the complexity of springtime ENSO evolution can be characterized by using a single ENSO index such as the Niño3.4 index or Trans-Niño index.

Given previous findings that ENSO may provide a source of seasonal predictability of US tornado outbreaks in spring [5, 8], there is a need to better characterize the springtime ENSO evolution and its link to US tornado activity. On this issue, a new method was recently presented to characterize the differences in space-time evolution of equatorial Pacific SSTAs during El Niño events [17]. An application of this method to the 21 El Niño events during 1949–2013 highlighted two leading orthogonal modes, which together explain more than 60% of the inter-event variance. The first

mode distinguishes a strong and persistent El Niño from a weak and early-terminating El Niño (figures 1(a) and (b)). A similar analysis applied to the 22 La Niña events during 1949–2013 also revealed two leading orthogonal modes, with the first mode distinguishing a resurgent La Niña from a transitioning La Niña (figures 1(c) and (d)).

The main objective of this study is to clarify the relationship between the springtime ENSO evolution and regional tornado outbreaks in the US. To achieve this and to advance our capability for developing a seasonal outlook for US tornado outbreaks, we first present a tornado density index, which can be used to measure the probability of tornado outbreaks within an area centered at a given geographic location. An outbreak is defined here as a sequence of 12 or more Fujita (F)-scale weighted F1–F5 tornadoes, occurring over five days within 200 km of a given location. Next, we use the tornado density index to explore the probability of tornado outbreaks in February–May in various regions of the US under the four main springtime ENSO behaviors (persistent versus early-terminating El Niño; resurgent versus transitioning La Niña) [17] and explain the associated atmospheric processes. We also report a potential link between the North Atlantic SST tripole and US regional tornado outbreaks in spring. Finally, we discuss further research that is needed to develop a seasonal outlook for springtime US tornado outbreaks.

2. Statistical methods and data used

To develop a seasonal outlook for US tornado outbreaks, it is important to understand exactly what a seasonal outlook can and cannot predict. First of all, tornadogenesis is a mesoscale problem [18]. Therefore, a seasonal outlook cannot pinpoint exactly when,

where and how many tornadoes may strike. Instead, the goal of a seasonal outlook is to predict in terms of probability which regions are more likely to experience a widespread outbreak of tornadoes.

To move forward with the goal of developing a seasonal outlook, we propose a tornado density index, which can be used to measure the probability that a tornado outbreak may occur in a predefined region. F0 tornadoes are excluded in our analysis to avoid a spurious long-term trend in the severe weather database [5, 19]. To avoid double-counting, the location and F-scale of each tornado are determined at the time when each tornado achieves its maximum F-scale. Additionally, the number of F1–F5 tornadoes is weighted in such a way that one Fn tornado is treated as n F1 tornadoes to put more emphasis on intense and violent tornadoes, similar to the destruction potential index [20]. The following steps describe a method to compute the proposed tornado density index, the threshold tornado density for an outbreak and the probability of US regional tornado outbreaks for 1950–2014.

The first step is to compute the daily tornado density index by counting the weighted number of F1–F5 tornadoes within a circle of 200 km radius from the center of each $1° \times 1°$ grid point for each day. Since a regional tornado outbreak may last up to 3–5 days, a moving window was used to accumulate the daily tornado density for five consecutive days. This is referred to as a 5 day overlapping tornado density index, or simply a tornado density (one value for each day and grid point).

The second step is to determine the threshold value of tornado density for a tornado outbreak. As shown in supplementary figure 1(a), the 99th percentile of the tornado density values averaged over the central and eastern US region, frequently affected by intense tornadoes ($30°–40°$ N and $100°–80°$ W), varies from 2 in August to 15 in April. For simplicity, the outbreak threshold in this study is set to a uniform value of 12, which is the average of the above values for March–May. Using the same procedure, but with the non-weighted tornado density, the outbreak threshold is reduced to 7 (supplementary figure 1(b)). Therefore, our definition of a tornado outbreak may be also interpreted as a sequence of 7 or more non-weighted tornado density within 5 days, which is quite consistent with previously used criteria that an outbreak should contain at least 6–10 F1–F5 tornadoes [20–22].

The final step is to identify months with one or more *outbreak days* (i.e., days in which the tornado density exceeds the outbreak threshold) for each grid point. For a given subset of data, the numbers of non-outbreak and outbreak months can be counted to compute the probability of US regional tornado outbreaks.

We used the severe weather database (http://www.spc.noaa.gov/wcm) to compute the tornado density index and probability of US regional tornado

outbreaks. The extended reconstructed sea surface temperature version 3b [23] was used to compute the leading modes of ENSO variability for the period of 1950–2014 [17]. The twentieth century reanalysis [24] was used to derive atmospheric anomalies, namely geopotential height at 500 hPa, moisture transport, low-level wind shear (850–1000 hPa), and convective available potential energy (CAPE), associated with the four dominant phases of springtime ENSO evolution. The National Centers for Environmental Prediction-National Center for Atmospheric Research reanalysis [25] was also used to derive variance of 5 day high-pass filtered meridional winds at 300 hPa, which was used to measure extratropical storm activity.
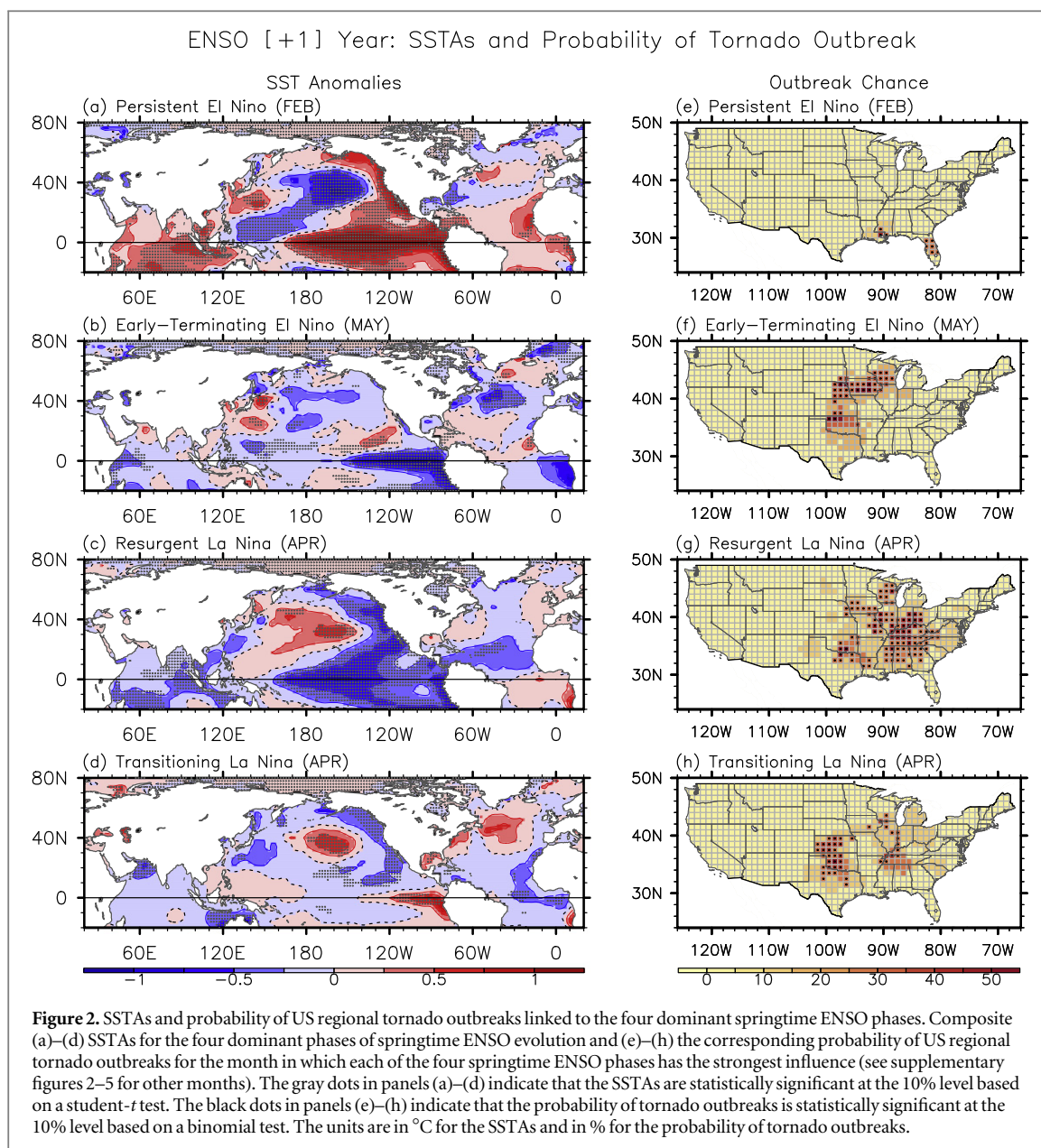
3. Results

3.1. Springtime ENSO phases and their links to US regional tornado outbreaks

The time-longitude plots of the tropical Pacific SSTAs, averaged over $5°$ S–$5°$ N, for the four most frequently recurring spatiotemporal ENSO evolution patterns [17] are presented in figure 1. The first case exhibits strong and positive SSTAs in the eastern tropical Pacific during the peak season persisting throughout spring ($+1$), and thus is referred to as a persistent El Niño (e.g, 1982–1983 El Niño); hereafter, any month/season in an ENSO onset year is denoted by the suffix (0), whereas any month/season in an ENSO decay year by the suffix ($+1$). The second case is characterized by relatively weak positive SSTAs in the central tropical Pacific during the peak season and an emergence of cold SSTAs in the eastern tropical Pacific shortly after the peak, and thus is referred to as an early-terminating El Niño (e.g., 1963–1964 El Niño). The third case describes a La Niña persisting into spring ($+1$) and evolving to another La Niña, and thus is referred to as a resurgent La Niña (e.g., 1998–1999 La Niña). This case is also frequently referred to as a two-year La Niña in the literature [26–28]. Finally, the fourth case describes a two-year La Niña transitioning to an El Niño, and thus is referred to as a transitioning La Niña (e.g., 1971–1972 La Niña).

Note that these four prominent spatiotemporal ENSO evolution patterns mainly describe ENSO evolution in spring ($+1$) following the peak of ENSO in winter. Thus, their ENSO phases in spring ($+1$) are referred to as the four dominant springtime ENSO phases. Both the resurgent and transitioning La Niña phases in spring ($+1$) are characterized by a positive zonal gradient of SSTAs from the central tropical Pacific to the eastern tropical Pacific, and thus are positive Trans-Niño phases [9, 10]. For more details on the atmosphere-ocean dynamics linked to the four dominant springtime ENSO phases, the reader is referred to reference [10].

The composite SSTAs for the four dominant phases of springtime ENSO evolution in February ($+1$)–

Figure 2. SSTAs and probability of US regional tornado outbreaks linked to the four dominant springtime ENSO phases. Composite (a)–(d) SSTAs for the four dominant phases of springtime ENSO evolution and (e)–(h) the corresponding probability of US regional tornado outbreaks for the month in which each of the four springtime ENSO phases has the strongest influence (see supplementary figures 2–5 for other months). The gray dots in panels (a)–(d) indicate that the SSTAs are statistically significant at the 10% level based on a student-*t* test. The black dots in panels (e)–(h) indicate that the probability of tornado outbreaks is statistically significant at the 10% level based on a binomial test. The units are in °C for the SSTAs and in % for the probability of tornado outbreaks.

May (+1) and the corresponding probability of regional tornado outbreaks are presented in supplementary figures 2–5. The climatological probability patterns of tornado outbreaks in February–May are also shown in supplementary figure 6. Figure 2 provides a summary of supplementary figures 2–5 highlighting the month in which each of the four springtime ENSO phases has the strongest influence on the probability of outbreaks. The gray dots indicate that the SSTAs are statistically significant at the 10% level (two-tailed) based on a Student's *t*-test. Similarly, the black dots mean that the probability of tornado outbreaks is statistically significant at the 10% level (one-tailed) based on the exact binomial test of the null hypothesis (i.e., the springtime ENSO phases have no effect on the probability of tornado outbreaks; see [29] about interpreting significance tests). For each case, we selected 6 to 8 actual ENSO events for the composite analysis based

on the sign and amplitude of the leading principal components of El Niño and La Niña variability (supplementary table 2).

As shown in supplementary figure 2(f), when a strong El Niño persists into spring (+1) after its peak (persistent El Niño), the probability of outbreaks is statistically indistinguishable from the climatological probability of outbreaks in March (+1) (supplementary figure 6(b)). This suggests that the outbreak frequency is overall unaffected or even suppressed in March (+1) by a strong El Niño persisting throughout spring (+1) [8]. However, the statistical significance of the reduction cannot be established since the frequency distribution of the outbreak chance is highly skewed to the right. Interestingly, there are small regions of significant increase in the probability of outbreaks in February (+1), April (+1) and May (+1). In particular, the probability of outbreaks increases

significantly over central Florida and limited regions of the gulf coast in February (+1) by up to 43%, and sporadically over the Ohio Valley and Northeast in April (+1) and May (+1) (figure 2(e) and supplementary figures 2(g) and 2(h); see supplementary figure 7 for the US climate regions).

When a weak El Niño terminates early and cold SSTAs develop over the eastern tropical Pacific in spring (+1) (early-terminating El Niño), there is no significant increase in the probability of outbreaks in February (+1) and March (+1) (supplementary figures 3(e) and (f)). However, in late spring especially in May (+1), the probability of outbreaks increases significantly up to 50% over the Upper Midwest (figures 2(b) and (f)).

When a La Niña persists into spring (+1) and evolves to another La Niña (resurgent La Niña), there is no significant increase in the probability of outbreaks in February (+1) and March (+1) (supplementary figures 4(e) and (f)). However, the probability of outbreaks surges significantly up to 57% in April (+1) over widespread regions in the Ohio Valley, Southeast and Upper Midwest, particularly Kentucky, Indiana, Iowa and Wisconsin (figure 2(g)) [8]. Note that the record-breaking 2011 tornado outbreaks occurred during a resurgent La Niña. Similarly, the Super Outbreak of 1974 occurred during a resurgent La Niña.

As shown in figure 2(d), when a two-year La Niña transitions to an El Niño (transitioning La Niña), the cold SSTAs in the central tropical Pacific are nearly dissipated away while the warm SSTAs in eastern tropical Pacific become strong and statistically significant in April (+1). In this case, the probability of tornado outbreaks increases strongly and significantly up to 50% in the South, particularly Kansas and Oklahoma, in April (+1) (figure 2(h)). In March (+1) some regions in the Ohio Valley are weakly but significantly increased in the probability of outbreaks (supplementary figure 5(f)).

Some important questions arise as to why the probability of US regional tornado outbreaks increases in spring following the peak of La Niña, and why the regions affected during the resurgent La Niña phase are quite different from the regions affected during the transitioning La Niña phase. Another important question is why the persistent and early-terminating El Niño phases are linked to the increased probability of outbreaks in different regions and different months. We attempt to address these questions next.

3.2. Springtime atmospheric variability over the US linked to ENSO phases
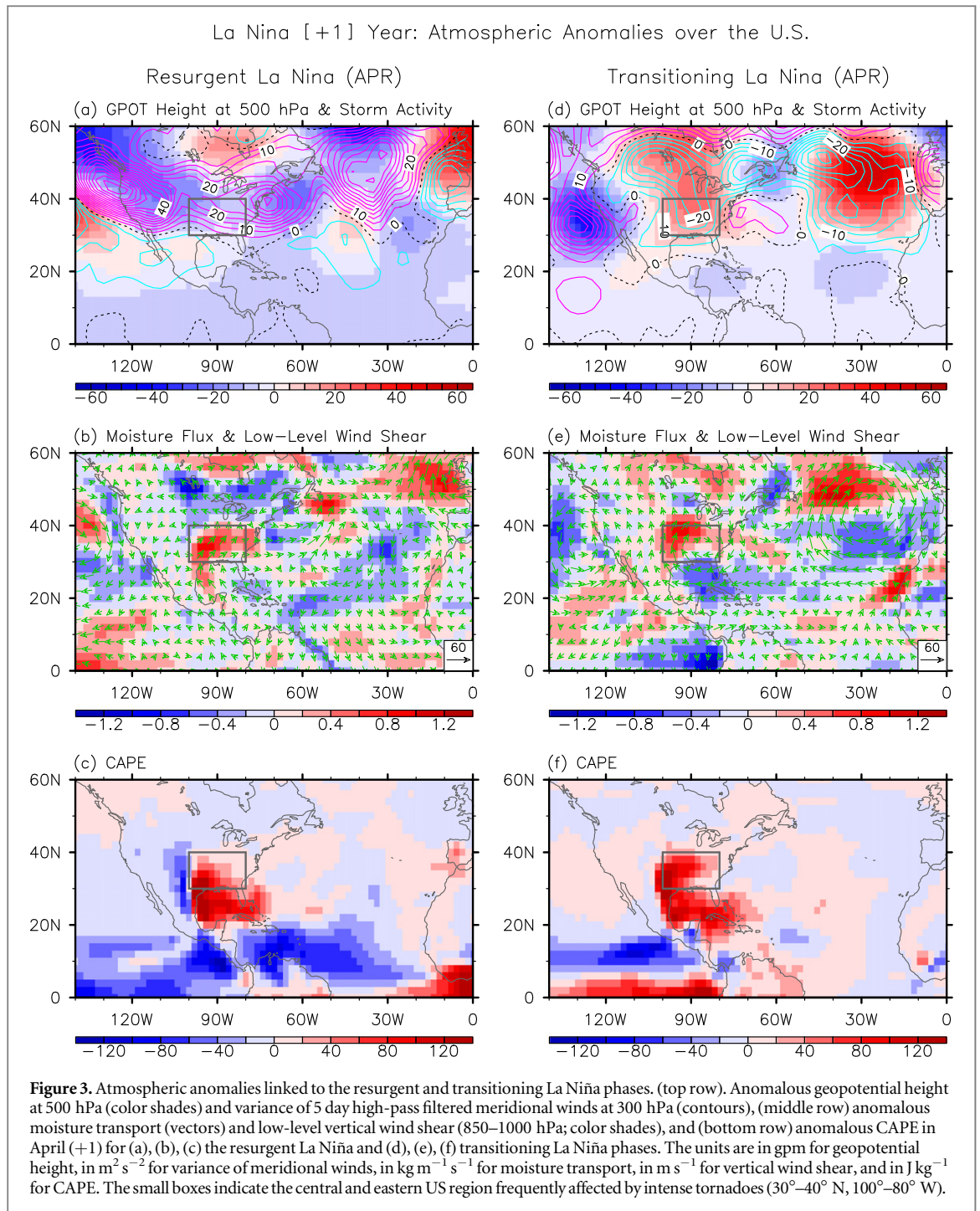
It is well known that La Niña causes the winter atmospheric jet stream to take an unusually wavy southeastward path into the US from southwestern Canada, thus bringing colder and drier upper-level air to the US. Hence, winter storm activity increases in the US particularly over the Ohio Valley [30]. As

illustrated in figure 3(a), during the resurgent La Niña phase in April (+1), an anomalous cyclone develops that brings colder and drier upper-level air to the US and thus increases the extratropical storm activity, suggesting that the typical La Niña weather conditions in winter persist into the resurgent La Niña phase in April (+1) [10]. The anomalous cyclone and the associated increase in equivalent barotropic winds in turn enhance the low-level vertical wind shear (850–1000 hPa) east of the Rockies, and increase and shift the stream of warm and moist air originating from the Gulf of Mexico more toward the east (figure 3(b)). The anomalous convergence of warm and moist air in turn increases CAPE east of the Rockies (figure 3(c)). As illustrated in earlier studies [2, 5, 31], these atmospheric anomalies produce a set of favorable atmospheric environments for tornado outbreaks in the Ohio Valley and Southeast, consistent with figure 2(g).

During the transitioning La Niña phase in April (+1), on the other hand, extratropical storm activity decreases east of the Rockies. Consistent with this feature, an anomalous anticyclone forms east of the Rockies, and induces anomalous southerly winds over the South (figure 3(d)). Therefore, the low-level vertical wind shear increases and the stream of warm and moist air from the Gulf of Mexico converges (figure 3(e)) increasing CAPE therein (figure 3(f)). These changes in the atmospheric environments during the transitioning La Niña phase in April (+1) are largely consistent with the increased probability of tornado outbreaks in the South (figure 2(h)).

The springtime large-scale atmospheric patterns during the persistent El Niño phase are largely opposite to those during the resurgent La Niña phase [10]. In particular, the atmospheric jet and storm track over the US shift southward; thus, the atmospheric environments over the central and northern US during the persistent El Niño phase in spring (+1) are largely unfavorable for tornado outbreaks [8]. However, the southward shifts of the atmospheric jet and storm track could also increase the low-level wind shear, moisture convergence and extratropical storm activity toward the southern US. As shown in figures 4(a) and (b), these changes in the atmospheric environments in the southern US are in line with the increased probability of outbreaks in central Florida during the persistent El Niño phase in February (+1) (figure 2(e)).

As shown in figure 4(d), an anomalous anticyclone forms over the northeastern US during the early-terminating El Niño phase in May (+1). Due to the associated equivalent barotropic wind anomalies, the stream of warm and moist air from the Gulf of Mexico to the Ohio Valley shifts toward the Upper Midwest (figure 4(e)). Also due to the equivalent barotropic wind anomalies associated with the anomalous anticyclone, the low-level wind shear and CAPE decrease over the Ohio Valley and increase over the Upper Midwest (figures 4(e) and (f)). These changes in the

Figure 3. Atmospheric anomalies linked to the resurgent and transitioning La Niña phases. (top row). Anomalous geopotential height at 500 hPa (color shades) and variance of 5 day high-pass filtered meridional winds at 300 hPa (contours), (middle row) anomalous moisture transport (vectors) and low-level vertical wind shear (850–1000 hPa; color shades), and (bottom row) anomalous CAPE in April (+1) for (a), (b), (c) the resurgent La Niña and (d), (e), (f) transitioning La Niña phases. The units are in gpm for geopotential height, in $m^2 s^{-2}$ for variance of meridional winds, in $kg\,m^{-1}\,s^{-1}$ for moisture transport, in $m\,s^{-1}$ for vertical wind shear, and in $J\,kg^{-1}$ for CAPE. The small boxes indicate the central and eastern US region frequently affected by intense tornadoes (30°–40° N, 100°–80° W).
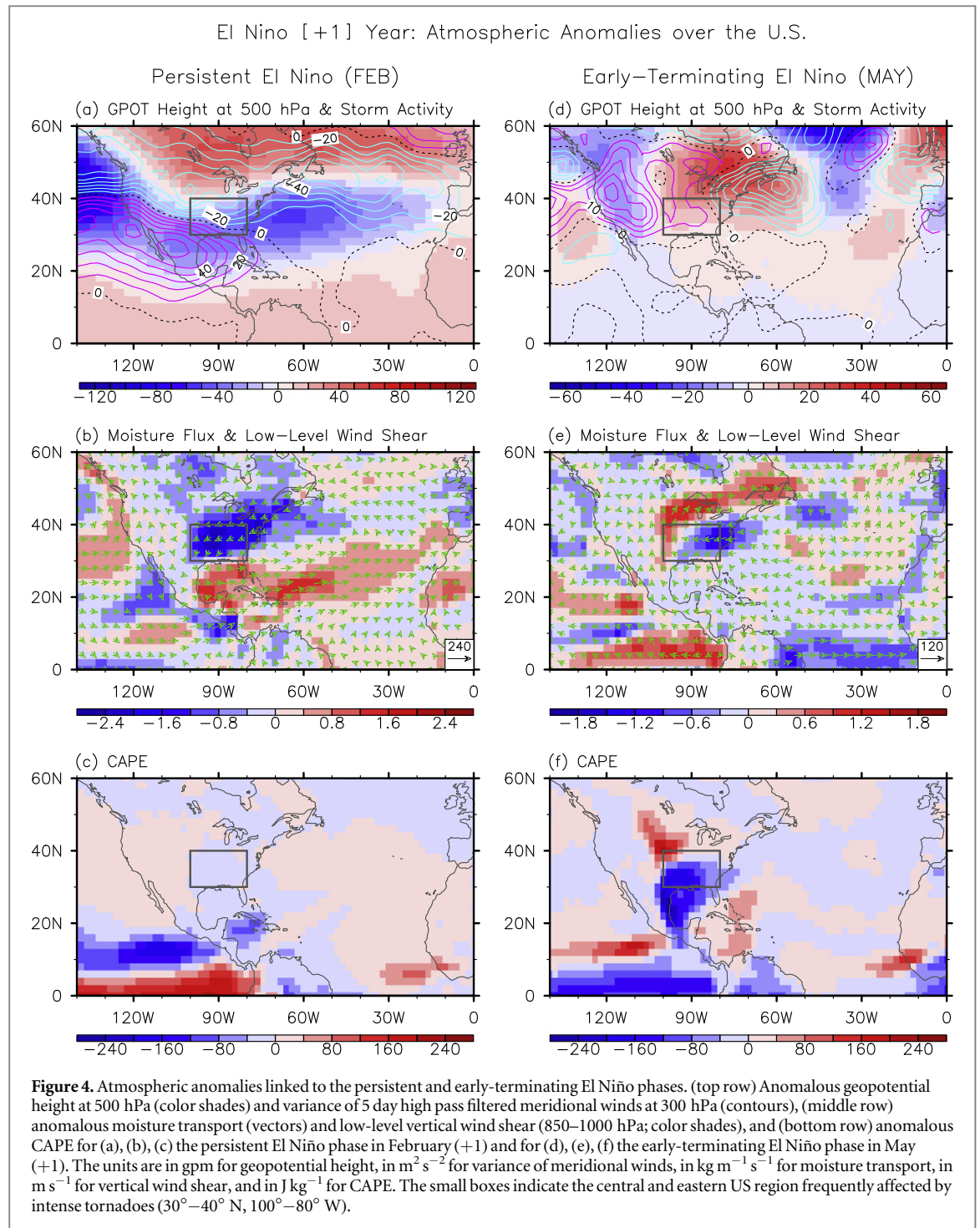
atmospheric environments during the early-terminating El Niño phase in May (+1) are quite consistent with the increased probability of tornado outbreaks in the Upper Midwest (figure 2(f)).

3.3. North Atlantic SST tripole and US regional tornado outbreaks

As shown in supplementary figure 8, there is a coherent and statistically significant pattern of springtime SSTAs in the North Atlantic in connection to the extreme US tornado outbreaks (supplementary table 3). This pattern is very similar to the North Atlantic SST tripole, which is the dominant mode of

interannual SST variability in the Atlantic in winter/spring and is known to be linked to multiple forcing mechanisms including the North Atlantic Oscillation and extratropical teleconnections from the tropics [32–37]. Hence, we further explore the potential link between the North Atlantic SST tripole and the probability of US regional tornado outbreaks. First, we performed an empirical orthogonal function (EOF) analysis of the detrended North Atlantic SSTAs in March–May and sorted the past 65 years based on the amplitude of the leading EOF mode. Then, we selected the most positive 16 cases (above upper quartile) and the most negative 16 cases (below lower quartile) from

Figure 4. Atmospheric anomalies linked to the persistent and early-terminating El Niño phases. (top row) Anomalous geopotential height at 500 hPa (color shades) and variance of 5 day high pass filtered meridional winds at 300 hPa (contours), (middle row) anomalous moisture transport (vectors) and low-level vertical wind shear (850–1000 hPa; color shades), and (bottom row) anomalous CAPE for (a), (b), (c) the persistent El Niño phase in February (+1) and for (d), (e), (f) the early-terminating El Niño phase in May (+1). The units are in gpm for geopotential height, in m² s⁻² for variance of meridional winds, in kg m⁻¹ s⁻¹ for moisture transport, in m s⁻¹ for vertical wind shear, and in J kg⁻¹ for CAPE. The small boxes indicate the central and eastern US region frequently affected by intense tornadoes ($30°-40°$ N, $100°-80°$ W).
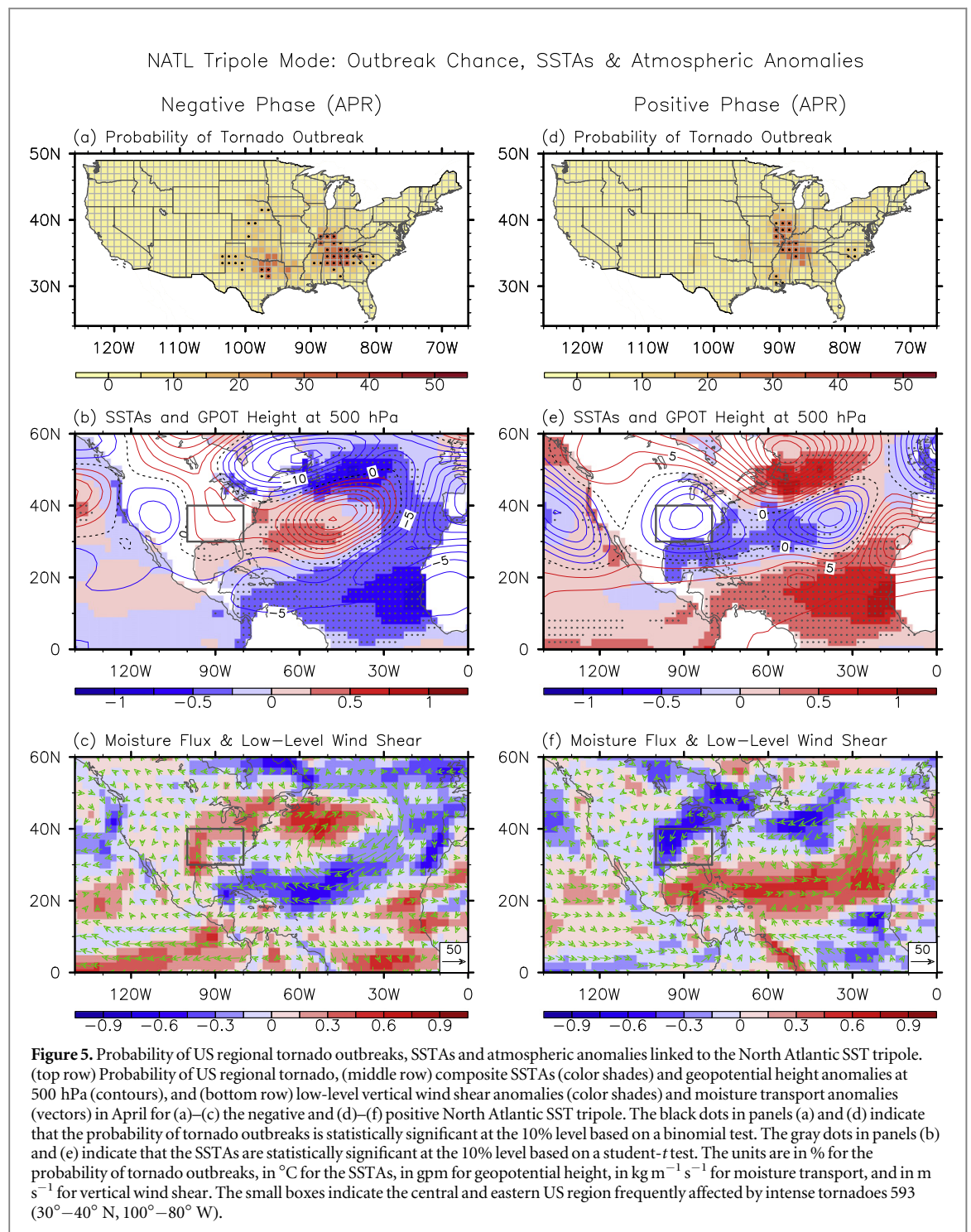
the sorted years to perform composite analysis (supplementary table 4).

As summarized in figure 5 and supplementary figure 9, the North Atlantic SST tripole is indeed linked to the probability of US regional tornado outbreaks in spring. During its negative phase (i.e., cold, warm and cold in the tropical, subtropical and subpolar North Atlantic, respectively), an anomalous anticyclone straddles the subtropical North Atlantic extending westward over the US. The associated increase in the equivalent barotropic winds along the western edge of the anomalous anticyclone enhances the low-level vertical wind shear and moisture convergence toward the South (figures 5(b) and (c)). As shown in supplementary figure 10(a), CAPE increases significantly over the Gulf of Mexico and the western North Atlantic. The anomalous anticyclone produces anomalous southeasterly winds across the gulf coast and the US east coast that in turn carry the extra moisture toward the Southeast and Ohio Valley (figure 5(c)). These changes in the low-level vertical wind shear, moisture convergence and CAPE are largely consistent with the significantly increased probability of tornado outbreaks over the South, Ohio

Figure 5. Probability of US regional tornado outbreaks, SSTAs and atmospheric anomalies linked to the North Atlantic SST tripole. (top row) Probability of US regional tornado, (middle row) composite SSTAs (color shades) and geopotential height anomalies at 500 hPa (contours), and (bottom row) low-level vertical wind shear anomalies (color shades) and moisture transport anomalies (vectors) in April for (a)–(c) the negative and (d)–(f) positive North Atlantic SST tripole. The black dots in panels (a) and (d) indicate that the probability of tornado outbreaks is statistically significant at the 10% level based on a binomial test. The gray dots in panels (b) and (e) indicate that the SSTAs are statistically significant at the 10% level based on a student-*t* test. The units are in % for the probability of tornado outbreaks, in °C for the SSTAs, in gpm for geopotential height, in kg m^{-1} s^{-1} for moisture transport, and in m s^{-1} for vertical wind shear. The small boxes indicate the central and eastern US region frequently affected by intense tornadoes 593 (30°−40° N, 100°−80° W).

Valley and Southeast (figure 5(a) and supplementary figures 9).

These relationships are nearly the opposite during the positive phase of the North Atlantic SST tripole (figures 5(d)–(f) and supplementary figures 9 and 10(b)). Interestingly, the probability of outbreaks significantly increases over the Ohio Valley in April during the positive phase of the North Atlantic SST tripole. Although the associated atmospheric anomalies do not provide a clear explanation for this increase, it appears that the stream of warm and moist air from the Gulf of Mexico to the South is somewhat shifted toward the Ohio Valley due to the anomalous cyclone over the US (figures 5(e) and (f)), which may offer an explanation for the increased probability of outbreaks in the Ohio Valley.

The results summarized in figure 5 are promising. However, it must be noted that a negative phase of the North Atlantic SST tripole forms more frequently in spring following the peak of La Niña [38] (supplementary table 4). Additionally, the mid-latitude components of the North Atlantic SST tripole largely respond to surface turbulent heat fluxes at seasonal time scale [39]. Therefore, it is unclear whether the North

Atlantic SST tripole adds much to the predictability of US regional tornado outbreaks.

Nevertheless, several studies have shown that the tropical component of the North Atlantic SST tripole could feedback on to the atmosphere aloft and thus could modulate the remote influence of ENSO on the atmospheric variability over the US [40–44]. Further studies using model experiments and advanced statistical methods are needed to clarify the impact of North Atlantic SST variability on the probability of US regional tornado outbreaks.

4. Discussion

This study illustrates the potential impacts of the dominant springtime ENSO phases and the North Atlantic SST tripole on the probability of US regional tornado outbreaks in spring. However, it is important to remember that a regional tornado outbreak may occur in any season and almost anywhere in the US regardless of ENSO state. For example, an unusual winter tornado outbreak occurred during the peak of the 2015–2016 El Niño. A similar winter tornado outbreak occurred during the peak of the 2000–2001 La Niña [45]. It is also important to remember that even during an overall quite season, one outbreak event could cause significant loss of life and property. Therefore, residents in the areas routinely exposed to severe weather systems should be ready for every severe weather season regardless of what a seasonal outlook may predict.

It should be clearly stated that the statistical analysis presented in this study does not constitute a prediction model or provide an actual predictive skill measure of tornado outbreak probability. To build a seasonal prediction model, additional steps are required. First, the EOF analysis of tropical Pacific SSTAs should be restricted only for February–May and applied for all years to better identify the leading orthogonal modes of springtime ENSO variability. Then, the first two principal components of springtime ENSO variability, which account for more than 75% of the total variance of tropical Pacific SSTAs (not shown), and the North Atlantic SST tripole mode in spring could be used as predictors of the monthly US regional tornado outbreak probability using a logistic regression analysis [46]. The regression coefficients obtained from the logistic regression analysis could be used to estimate the probability of US regional tornado outbreaks given the amplitudes of the three predictors. Combining this statistical tool with a dynamic seasonal forecast model, which could be used to obtain the three predictors with 1–3 months lead time, it may be possible to build a seasonal outlook for US regional tornado outbreaks. A cross validation should be performed to evaluate the actual predictive skill of a such seasonal outlook. To this end, it is quite promising that high-resolution climate models are now beginning to demonstrate skill in simulating and predicting seasonal variations in some of the elements critical to US tornado outbreaks [11, 47, 48].

Acknowledgments

References

[1] Tippett M K, Allen J T, Gensini V A and Brooks H E 2014 Climate and hazardous convective weather *Curr. Clim. Change Rep.* **1** 60–73

[2] Tippett M K, Sobel A H and Camargo S J 2012 Association of US tornado occurrence with monthly environmental parameters *Geophys. Res. Lett.* **39** L02801

[3] Weaver S J, Baxter S and Kumar A 2012 Climatic role of North American low-level jets on US regional tornado activity *J. Clim.* **25** 6666–83

[4] Barrett B S and Gensini V A 2013 Variability of central United States april–may tornado day likelihood by phase of the Madden–Julian oscillation *Geophys. Res. Lett.* **40** 2790–5

[5] Lee S-K, Atlas R, Enfield D B, Wang C and Liu H 2013 Is there an optimal ENSO pattern that enhances large-scale atmospheric processes conducive to major tornado outbreaks in the US? *J. Clim.* **26** 1626–42

[6] Thompson D B and Roundy P E 2013 The relationship between the Madden–Julian Oscillation and US violent tornado outbreaks in the spring *Mon. Weather Rev.* **141** 2087–95

[7] Elsner J B and Widen H W 2014 Predicting spring tornado activity in the central Great Plains by 1 March *Mon. Weather Rev.* **142** 259–67

[8] Allen J T, Tippett M K and Sobel A H 2015 Influence of the El Nino/Southern Oscillation on tornado and hail frequency in the United States *Nat. Geosci.* **8** 278–83

[9] Trenberth K E and Stepaniak D P 2001 Indices of El Niño evolution *J. Clim.* **14** 1697–701

[10] Lee S-K, Mapes B E, Wang C, Enfield D B and Weaver S J 2014 Springtime ENSO phase evolution and its relation to rainfall in the continental US *Geophys. Res. Lett.* **41** 1673–80

[11] Krishnamurthy L, Vecchi G A, Msadek R, Wittenberg A, Delworth T L and Zeng F 2015 The seasonality of the Great Plains low-level jet and ENSO relationship *J. Clim.* **28** 4525–44

[12] Muñoz E and Enfield D B 2011 The boreal spring variability of the Intra-Americas low-level jet and its relation with precipitation and tornadoes in the eastern United States *Clim. Dyn.* **36** 247–59

[13] Chiang J C H and Vimont D J 2004 Analogous Pacific and Atlantic meridional modes of tropical atmosphere–ocean variability *J. Clim.* **17** 4143–58

[14] Yu J-Y and Kim S T 2010 Three evolution patterns of central-pacific El Niño *Geophys. Res. Lett.* **37** L08706

[15] Yeh S-W, Kug J-S and An S-I 2014 Recent progress on two types of El Niño: observations, dynamics, and future changes *Asia-Pac. J. Atmos. Sci.* **50** 69–81

[16] Capotondi A *et al* 2015 Understanding ENSO diversity *Bull. Am. Meteorol. Soc.* **96** 921–38

[17] Lee S-K, Mapes B E, Wang C, Enfield D B and Weaver S J 2014 Spring persistence, transition and resurgence of El Niño *Geophys. Res. Lett.* **41** 8578–85

[18] Doswell C A III and Bosart L F 2001 Extratropical synoptic-scale processes and severe convection *Severe Convective Storms* ed C A Doswell III (Boston, MA: American Meteorological Society)

[19] Verbout S M, Brooks H E, Leslie L M and Schultz D M 2006 Evolution of the US tornado database: 1954–2003 *Weather Forecast.* **21** 86–93

[20] Doswell C A III, Edwards R, Thompson R L, Hart J A and Crosbie K C 2006 A simple and flexible method for ranking severe weather events *Weather Forecast.* **21** 939–51

[21] Galway J G 1977 Some climatological aspects of tornado outbreaks *Mon. Weather Rev.* **105** 477–84

[22] Fuhrmann C M *et al* 2014 Ranking of tornado outbreaks across the United States and their climatological characteristics *Weather Forecast.* **29** 684–701

[23] Smith T M, Reynolds R W, Peterson T C and Lawrimore J 2008 Improvements to NOAA's historical merged land-ocean surface temperature analysis (1880–2006) *J. Clim.* **21** 2283–96

[24] Compo G P *et al* 2011 The twentieth century reanalysis project *Q. J. R. Meteorol. Soc.* **137** 1–28

[25] Kalnay E *et al* 1996 The NCEP/NCAR 40-year reanalysis project *Bull. Am. Meteorol. Soc.* **77** 437–71

[26] Okumura Y M and Deser C 2010 Asymmetry in the duration of El Niño and La Niña *J. Clim.* **23** 5826–43

[27] Okumura Y M, Ohba M, Deser C and Ueda H 2011 A proposed mechanism for the asymmetric duration of El Niño and La Niña *J. Clim.* **24** 3822–9

[28] DiNezio P N and Deser C 2014 Nonlinear controls on the persistence of La Niña *J. Clim.* **27** 7335–55

[29] von Storch H and Zwiers F W 2001 *Statistical analysis in climate research* (Cambridge: Cambridge University Press)

[30] Eichler T and Higgins W 2006 Climatology and ENSO-related variability of North American extratropical cyclone activity *J. Clim.* **19** 2076–93

[31] Brooks H E, Lee J W and Cravenc J P 2003 The spatial distribution of severe thunderstorm and tornado environments from global reanalysis data *Atmos. Res.* **67–8** 73–94

[32] Xie S-P and Tanimoto Y 1998 A pan-Atlantic decadal climate oscillation *Geophys. Res. Lett.* **25** 2185–8

[33] Okumura Y, Xie S-P, Numaguti A and Tanimoto Y 2001 Tropical Atlantic air–sea interaction and its influence on the NAO *Geophys. Res. Lett.* **28** 1507–10

[34] Peng S, Robinson W A and Li S 2002 North Atlantic SST forcing of the NAO and relationships with intrinsic hemispheric variability *Geophys. Res. Lett.* **29** 1171–4

[35] Wu L, He F, Liu Z and Li C 2007 Atmospheric teleconnections of tropical Atlantic variability: interhemispheric, tropical–extratropical, and cross-basin interactions *J. Clim.* **20** 856–70

[36] Schneider E K and Fan M 2012 Observed decadal North Atlantic tripole SST variability : II. Diagnosis of mechanisms *J. Atmos. Sci.* **69** 51–64

[37] Yu B and Lin H 2016 Tropical atmospheric forcing of the wintertime North Atlantic Oscillation *J. Clim.* **29** 1755–72

[38] Lau N-C and Nath M J 2001 Impact of ENSO on SST variability in the North pacific and North Atlantic: Seasonal dependence and role of extratropical sea–air coupling *J. Clim.* **14** 2846–66

[39] O'Reilly C H, Huber M, Woollings T and Zanna L 2016 The signature of low frequency oceanic forcing in the Atlantic Multidecadal Oscillation *Geophys. Res. Lett.* **43**

[40] Sutton R T and Hodson D L R 2007 Climate response to basin-scale warming and cooling of the North Atlantic Ocean *J. Clim.* **20** 891–907

[41] Lee S-K, Wang C and Mapes B E 2009 A simple atmospheric model of the local and teleconnection responses to tropical heating anomalies *J. Clim.* **22** 272–84

[42] Mo K C, Schemm J-K E and Yoo S-H 2009 Influence of ENSO and the Atlantic Multidecadal Oscillation on drought over the United States *J. Clim.* **22** 5962–82

[43] Wang C, Lee S-K and Enfield D B 2008 Climate response to anomalously large and small Atlantic warm pools during the summer *J. Clim.* **21** 2437–50

[44] Weaver S J, Schubert S and Wang H 2009 Warm season variations in the low-level circulation and precipitation over the central United States in observations, AMIP simulations, and idealized SST experiments *J. Clim.* **22** 5401–20

[45] Cook A R and Schaefer J T 2008 The relation of El Niño—Southern Oscillation (ENSO) to winter tornado outbreaks *Mon. Weather Rev.* **136** 3121–37

[46] Cox D R 1958 The regression analysis of binary sequences (with discussion) *J. R. Stat. Soc.* B **20** 215–42

[47] Yang X *et al* 2015 Seasonal predictability of extratropical storm tracks in GFDL's high-resolution climate prediction model *J. Clim.* **28** 3592–611

[48] Jia L *et al* 2015 Improved seasonal prediction of temperature and precipitation over land in a high-resolution GFDL climate model *J. Clim.* **28** 2044–62